Rigid Rod Conjugated Polymers for Nonlinear Optics. 1. Characterization and Linear Optical Properties of Poly(aryleneethynylene) Derivatives

M. Moroni and J. Le Moigne*

Groupe des Matériaux Organiques, Institut de Physique et Chimie des Matériaux de Strasbourg, UM 46 (CNRS-ULP), 6, Rue Boussingault, Strasbourg, 67083 Cedex, France

S. Luzzati

CNR, Istituto Di Chimica Delle Macromolecole, Via Bassini 15, 20133 Milano, Italy

Received June 3, 1993; Revised Manuscript Received September 29, 1993®

ABSTRACT: New rigid rod and conjugated polymers based on poly(aryleneethynylene) have been synthesized by a palladium-catalyzed polycondensation. Long alkyl side chains were bound to the aryl groups by ester, ether, or other functions in order to increase solubility, in order that this might lead to higher molecular weights and longer conjugated backbones. We chose also to act on the electron density of the conjugated chain by means of an electroactive functional group or an electron donor or electron acceptor attached to the phenyl moiety. We first synthesized some polymers with alkoxy groups and long hydrocarbon tails of 10 and 12 carbon atoms. We compared these model polymers with other polymers, homopolymers based on phenyl groups bearing thioether substituents or alkyl esters as electron acceptors, and also alternated copolymers based on the former and other electron donors, anthryl or thienyl groups, or acceptors, phenyl substituted by ester or nitro groups. The characterization by GPC of the poly(phenyleneethynylene) substituted with two dodecyl ether chains on the phenyl group shows the highest average molecular weight ever synthesized on this type of homopolymer, finding a value as high as 10^5 g/mol. The new homopolymers and copolymers based on the phenyl alkyl ether were similarly characterized. The spectroscopic linear properties in solution and in solid thin films confirm a large shift of the main absorption peak of the π-π^* transition in the visible range according to the donor or acceptor character of the substituent or comonomer group. Studies by Raman spectroscopy of the alkoxy phenyl homopolymer and the corresponding trimer show a shift of the triple bond stretching band and thus a greater delocalization for the polymer. Highly birefringent liquid crystalline phases are induced by rubbing or shearing and are confirmed by an observation of the optical dichroism along the shearing direction.

1. Introduction

The linear and rigid conjugated chains of polymers have attracted our attention for the preparation and the study of processable polymers for nonlinear optical applications.[1] The processing of conjugated polymers into films or fibers will be crucial for the development of nonlinear materials for photonics applications. Unfortunately, the polarizable π electrons of rigid rod conjugated polymers lead to strong intermolecular interaction, and macromolecules of high molecular weight are often insoluble and infusible. The processing of conjugated polymers has also been developed in the field of conducting polymers. The solubility of rigid rod conjugated polymers such as poly(*p*-phenylene) is increased if one or two alkyl chains are tied to the repeating units.[2] Other highly interesting compounds have been developed based on rigid rod conjugated polymers, which combine the properties of aryl and acetylenic functions leading to a new family of linear or bidimensional polymers.[3,4] The idea of using the alternating aryl and ethynyl group in the main chain of a polymer was introduced 10 years ago.[5] The first synthetic route to the polymerization of the arylethynyl was performed via a cuprous acetylide. Recently, a more convenient method using the palladium-catalyzed polycondensation has been applied to the synthesis of aryl ynylene polymeric chains,[6] more generally known in organic synthesis as a Heck coupling.[7] During the catalytic reaction either the low solubility of the arylethynyl oligomers or more likely the low solubility of the intermediate complex prevents the formation of high molecular weight chains. The molecular weights of the series containing phenyl, anthryl, thienyl, or pyridyl moieties[3] rose only to values between 1500 and 4000. Recently, the possibility of increasing the solubility and simultaneously the molecular weight of such backbones was investigated by the attachment of flexible side chains to the rigid core of the main chain.[6] The molecular weights of these polymers, characterized by the classical methods such as GPC or vapor pressure osmometry, did not rise above a value greater than 10^4 (DPn about 15) for the more soluble homopolymer with C18 alkoxy groups.

In this work we chose to attach an alkyl chain on the aryl by the intermediate ester or ether function groups in order to increase the solubility and the molecular weight. Long chains of poly(aryl ynylene) were obtained by improving the polymerization conditions. We chose also to act on the electron density of the conjugated chain by means of an electroactive functional group, electron donor or electron acceptor attached on the phenyl moiety. We synthesized, first, some polymers with alkoxy groups and long hydrocarbons tails of 10 and 12 carbon atoms. These polymers will act as reference for the comparison with polymers based on electron donors, anthryl or thienyl groups, or electron acceptors as esters with different lengths and different numbers of paraffinic tails. In this work we will give a large characterization of these new polymers by a GPC chromatographic study related to spectroscopic linear properties in solution and in solid thin films, including true molecular weight determinations obtained by on-line light scattering.

2. Results

2.1. Synthetic Methods. The phenylene ynylene polymers were synthesized by a condensation method known as Heck coupling,[8-10] A substituted diethynyl arene

® Abstract published in *Advance ACS Abstracts*, December 15, 1993.

0024-9297/94/2227-0562$04.50/0 © 1994 American Chemical Society

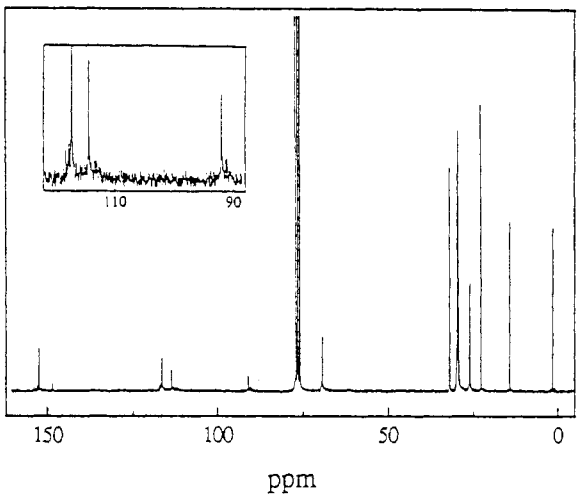

Figure 1. ^{13}C NMR spectra of pPYOC12 in $CDCl_3$.

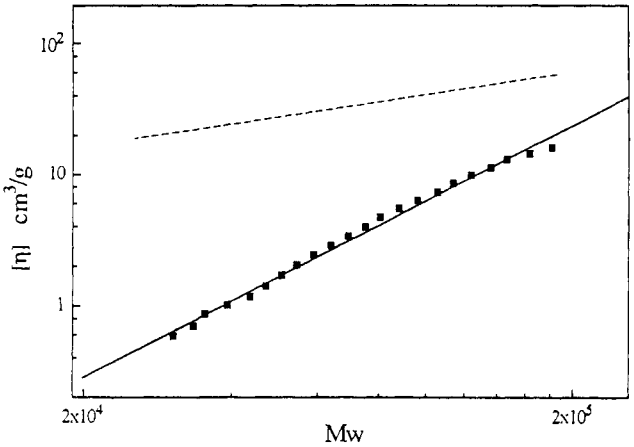

Figure 2. Intrinsic viscosity vs M_w of pPYOC12. The continuous line represents the least-squares fit of the intrinsic viscosity of the polymer, the dotted line the curve of the polystyrene.

reacts with a disubstituted halogenoaryl compound in the presence of a catalytic amount of a palladium complex. This general route is described as follows

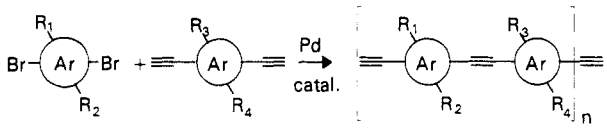

where R_1, R_2, R_3, R_4 could be the same or different (H, NO_2, alkyl ether, alkyl thioether, or alkyl ester...). As aryl units we synthesized homo- or copolymers with phenyl, thienyl, anthryl, or stilbene groups. The polymers and their polymerization yields are given in Table 1, where we also report the abbreviated names used in this paper.

2.2. Properties of the Polymers. All these polymers are deep colored from yellow to purple red; they are soluble in solvents such as THF, CH_2Cl_2, $CHCl_3$, hot toluene, and xylene. Those with acceptor substituents (ester, NO_2) show poor solubilities, except in THF, which could be considered as the best solvent. pPYOC12A is slightly soluble, except in hot toluene and xylene.

2.2.1. Characterization of the Polymers in Solution. NMR Spectroscopy. The ^1H and ^{13}C NMR spectra were obtained in $CDCl_3$. The ^1H spectra of the polymers are slightly different from those of the monomers. All the resonances are broader, and no signal has been detected in the near 3.5 ppm region of the acetylenic proton in any case. A very weak additional signal appears in the aromatic region (at 7.10 ppm for pPYOC12), which is assigned to the phenyl end groups, carrying a nonreactive bromine atom.

Figure 1 represents the ^{13}C spectra of pPYOC12. It shows a signal at 92 ppm, assigned to the acetylenic carbons. The aromatic carbons of the main chains are detected at 153, 117, and 114 ppm. The small peak at 149 ppm might be assigned to the terminal carbons of the chain end. The carbons belonging to the alkoxy side chains appear as very strong signals, at 70 and from 32 to 14 ppm. The triplet at 77 ppm is due to $CDCl_3$. The ^{13}C spectra of the other polymers show similar signals.

Molecular Weight and Stiffness. The molecular weight measurements were performed by gel permeation chromatography (GPC) in eluent THF using the coupled on line light-scattering technique.[11] By this method the true molecular weights of the rigid rod polymers can be obtained versus the elution volume. A complete molecular weight distribution study was performed on the homopolymer phenyl diether C12 (pPYOC12). Very high molecular weights have been detected, values as high as 4.5×10^5, and the weight-average molecular weight of the sample raised $\bar{M}_w = 9.8 \times 10^4$, taking a refractive index increment in THF of 0.264×10^{-3} $m^3 \cdot kg^{-1}$. Moreover, the molecular weight distribution $\bar{M}_w/\bar{M}_n = 1.47$ is not very broad for this type of polycondensation. Calculated from a single measurement of light scattering on a sample, we found a value of the weight average molecular weight $\bar{M}_w = 10.5 \times 10^4$, which confirms the GPC determination and proves that the column acts only by a size exclusion process without absorption of the rigid and highly polarizable chain. All the polymers of Table 1 were also checked by GPC, which shows the same typical shape of the chromatogram as pPOC12 with a maximum peak in the same range of elution volume (V_{el}). According to the elution law $\bar{M}_w = fV_{el}$ of this polymer type, this observation implies that the weight average molecular weights $\bar{M}_w$ for the remaining polymers of the series are found in the range of (8–10) $\times 10^4$. Using the GPC preparative method on the crude product, we removed the shortest oligomers (dimers or trimers) of the samples, which should be inactive for nonlinear optics (NLO) and for all following measurements.

By using the universal law of the variation of the hydrodynamic volume versus the elution volume in the chromatogram, the intrinsic viscosity $[\eta]$ of the polymer can be related to the light-scattering molecular weight. Figure 2 shows the curve $\log [\eta] = f(\log M_w)$ for polymer pPYOC12. The linear plot in this log–log representation shows that the polymer in solution obeys the Mark Houwink equation, $[\eta] = KM^\alpha$, where a high value of $\alpha = 1.92$ is calculated. This high value of the power α shows a very high stiffness of the polymer chain in solution, which confirms the rigid rod character of this type of backbone.[12a,b]

The very high value of the radius of gyration $\langle R_g \rangle$, calculated from the Zimm plot, is 630 Å, a value which is perfectly consistent with the rigid rod character of the polymer and the high stiffness of the chain in solution.

2.2.2. Optical Properties. UV-Vis Spectra. Figure 3a shows the UV–vis spectra of pPYOC10 and the corresponding diethynyl monomer in THF solution. The polymer, unlike the monomer, shows an important absorption in the visible range with a peak at 429 nm. The spectra in solution of the three parent homopolymers and the alternated copolymer, pPYOC10, pPYCOOC12, and cpPYOC12A are given in Figure 3b. The spectra have similar features: a main peak with a maximum between 380 and 510 nm and a small peak in the near-UV, around

Table 1. Spectroscopic Data of Solutions or of Thin Isotropic Solid Films for the Principal Poly(aryl ynylenes)

polymers	polym yield (%)	λ_{max} soln THF (nm)	ϵ (L·mol^{-1})	λ_{max} film (nm)
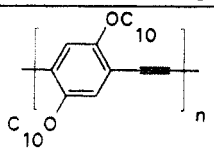 pPYOC10	72	429	1.64×10^4	455 2.72 eV
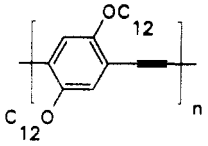 pPYOC12	75	425	1.63×10^4	453 2.73 eV
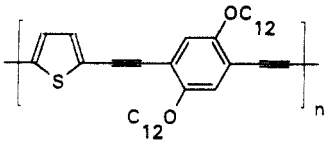 cpPYOC12T	74	433	1.02×10^4	450 2.75 eV
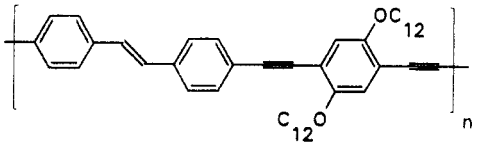 cpPYOC12S	38	425	1.58×10^4	469 2.64 eV
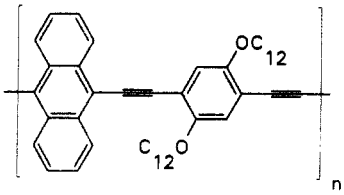 cpPYOC12A	68	508	7.1×10^3	521 2.38 eV
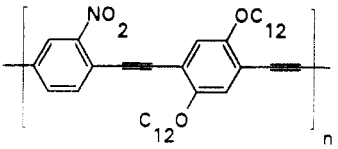 cpPYOC12N	39	404	1.14×10^4	412 3.00 eV
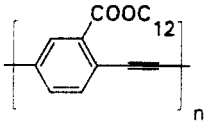 pPYCOOC12	65	383	3.62×10^4	405 3.06 eV
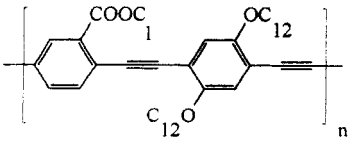 cpPYCOOC12C1	52	408	2.84×10^4	412 3.00 eV
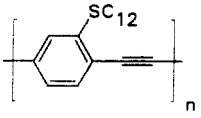 pPYSC12	55		1.70×10^4	

310 nm. The spectra of the solid films are almost the same as in solution, but with a red shift of the main peak of about 15 nm.

Passing from pPYOC12, where the lateral side chains are donor (ether substituents) to pPYCOOC12, where the side chains are acceptor (ester groups), Figure 3c shows

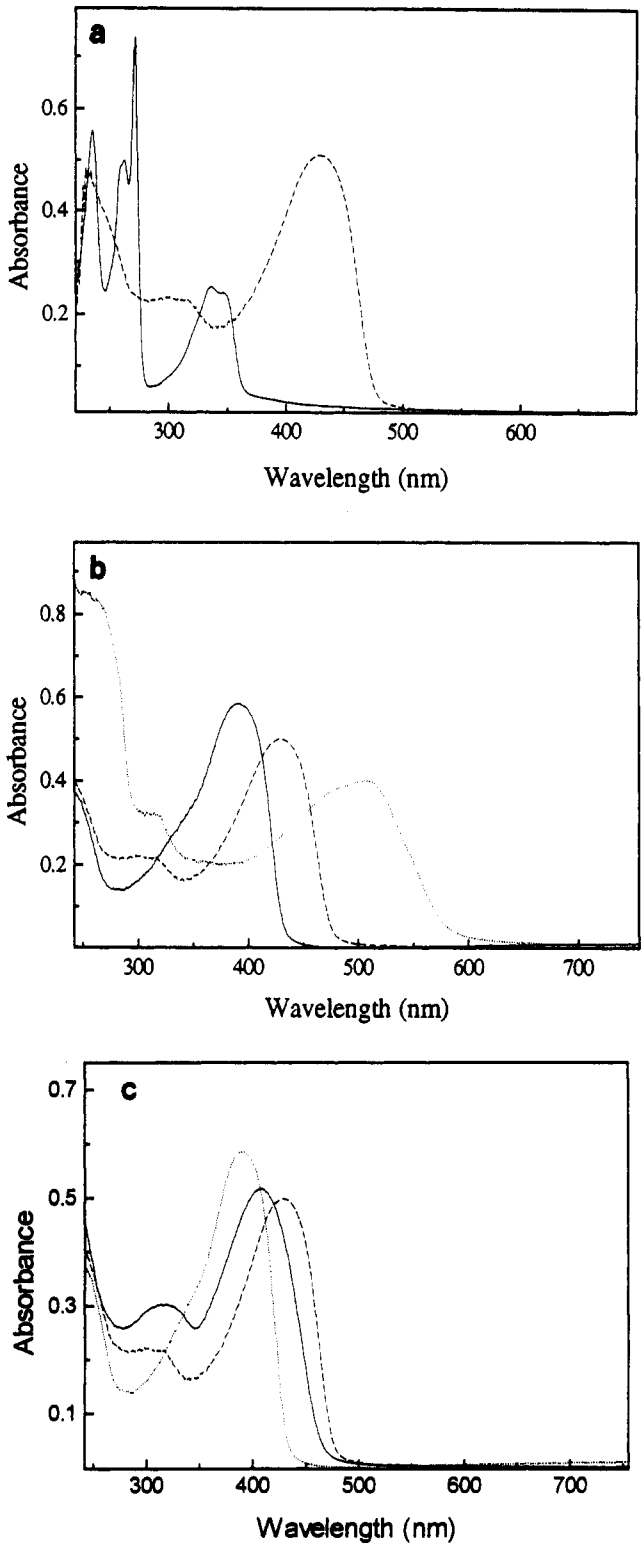

Figure 3. UV–vis spectra in THF (a) of the monomer unit PYOC10 (continuous line) and the corresponding polymer pPYOC10 (dashed line), (b) of the pPYCOOC12 (continuous line), pPYOC10 (dashed line), and cpPYOC12A (dotted line), and (c) of the pPYCO2C12 (dotted line), cpPYCOOC12 (continuous line), and pPYOC12 (dashed line).

a net blue shift of the absorption peak, from 431 nm for pPYOC12 to 383 nm for pPYCOOC12, i.e., $\Delta\lambda_{max}$ = 48 nm. The λ_{max} values of the solutions in THF and of the solid-state films are given in Table 1 for the polymers of the diethynyl series.

pPYSC12 has a broad absorption band from 300 to 450 nm with a band at 335 nm and a shoulder at 390 nm; it shows an orange color which is due to its strong luminescence. The copolymer cpPYCOOC12 having alternated ether and ester substituents has a peak at 408 nm, which is not so far from the average value of the pure ester and pure ether homopolymer λ_{max}. The other copolymer with alternated donor and acceptor substituents (ether–nitrobenzene copolymer) shows similar behavior with a λ_{max} = 404 nm. The intramolecular charge transfer is well known for phenyl derivatives. The delocalization is greater with a donor than with an acceptor, the former giving a more efficient charge transfer to the conjugated chain through the phenyl ring.

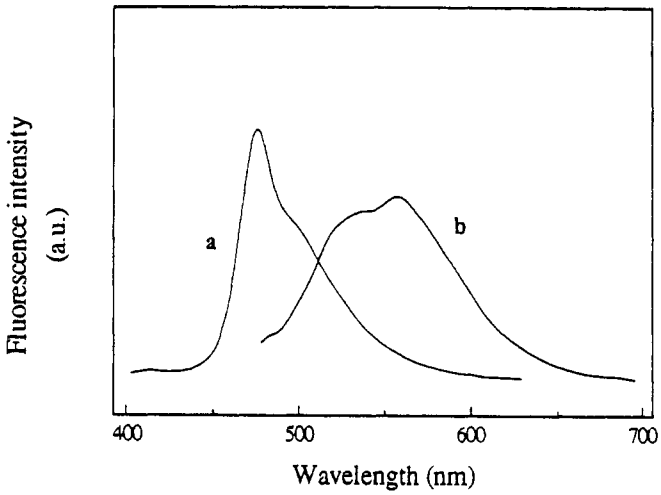

Figure 4. Fluorescence spectra of pPYOC12 in THF solution (a) and in solid state (b).

The copolymer spectra with ether substituents and stilbene or thiophene units related to the ether homopolymer shows only little differences. A notable exception takes place for the copolymer phenyl–ether–anthracene which shows a large red shift of about 83 nm with the main peak at 508 nm.

Fluorescence. The polymers of this series have a very intense fluorescence in solution (green) even at a very low concentration and in solid state (yellow). Figure 4 shows, for example, the fluorescence of the homopolymer pPYOC12 in solid state and dissolved in THF (4×10^{-7} mol/L). The solid presents a maximum emission peak at 558 nm with the excitation wavelength at 453 nm and the solution at 473 nm with the excitation wavelength at 300 nm.

Raman Spectroscopy. The Raman spectra were obtained at room temperature on cast films of the polymer ether pPYOC12, the oligomer model $(PYOC12)_3$, and the thioether pPYSC12. The measurements were obtained with a 1064-nm excitation wavelength in order to avoid the strong luminescence of these samples in the visible region.

The Raman spectra of the three samples are compared in Figure 5. Figure 5a shows the spectra of the pPYOC12 trimer and polymer; the trimer shows several bands which disappear in the polymer, where few bands are observed at 2196, 1595, 1548, 1288, 1069, and 800 cm^{-1}. Such a phenomenon is common to all the known classes of polyconjugated oligomers and polymers: the A_g modes which are coupled to the π–π^* electronic transition increases their relative intensity in the spectrum with conjugation, even when the spectra are obtained far from resonance. The 2196 cm^{-1} band is associated with a mode containing a strong C≡C stretching component; the 1600 cm^{-1} doublet is associated with vibrational modes of the conjugated backbone containing ring deformations and aryl ethynyl C–C stretching vibrations.

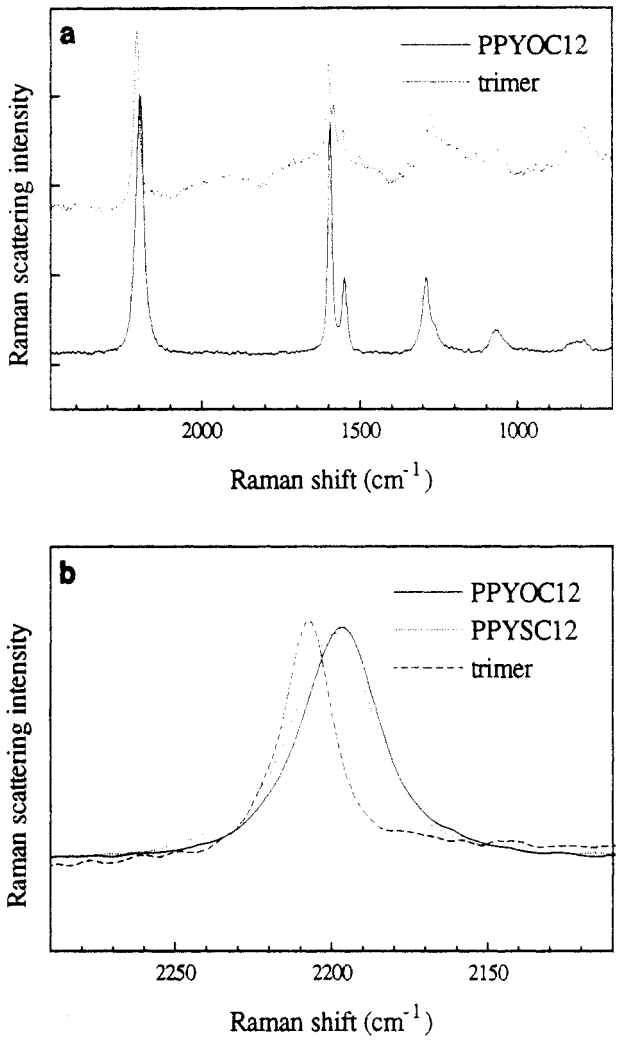

Figure 5. Raman scattering spectra (a) of the pPYOC12 (continuous line), and the corresponding trimer $(PYOC12)_3$ (dotted line) and (b) of pPYOC12 (continuous line), pPYSC12 (dotted line), and the $(PYOC12)_3$ trimer (dashed line).

Figure 5b shows the C≡C stretching band of the three samples. There is a shift to lower frequencies passing from the trimer ($\Delta\nu$ = 2207 cm^{-1}) to the polymer ($\Delta\nu$ = 2196 cm^{-1}) while the bands below 2000 cm^{-1} do not vary in frequency. This shift is due to an increase in the polymer of π electron delocalization along the unsaturated chain,[13a] which has been also detected in the UV–vis absorption spectra by a red shift of 48 nm. The polymer shows a broader C≡C stretching band (30 cm^{-1} half-height band width for pYOC12, 19 cm^{-1} for $(PYOC12)_3$), thus indicating the presence in the polymeric sample of a wider distribution of conjugation lengths. pPYSC12 and pPYOC12 show a similar C≡C stretching band ($\Delta\nu$ = 2199 cm^{-1} and 35 cm^{-1} half-height band width for pPYSC12) which may be roughly interpreted as a similar mean conjugation length for both polymers, with a wider polydispersity in pPYSC12.

In conclusion, these results indicate that the Raman C≡C stretching band frequency is a probe of the π-electron delocalization along the conjugated backbone, while similar to poly(*p*-phenylenevinylene),[13b] the Raman modes below 2000 cm^{-1} do not shift in frequency with the extent of conjugation.

2.2.3. Thermal Properties. We studied the behavior of two homopolymers, the first with one ester substituent on each phenyl (pPYCOOC12) and the second disubstituted with ether side chains (pPYOC12). By thermogravimetric analysis performed in air (Figure 6), we observed for the pPYCOOC12 a weight loss of 2% at 180 °C. The loss increased after 200 °C and became faster after 350 °C. The remaining weight at 800 °C was about 25%. The pPYOC12 showed a better thermal stability than the monoester (2% weight loss at 220 °C).

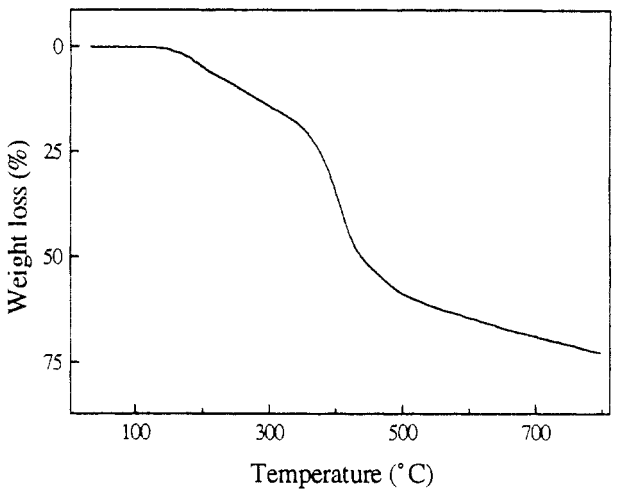

Figure 6. Thermogravimetric analysis of pPYCOOC12 in air.

The solid films of those polymers, obtained by casting the concentrated solutions on glass plates, were observed in polarized light. Only a homeotropic orientation was detected. Nevertheless, these films exhibited a strong birefringence after rubbing the surface or shearing the melt. This birefringence could still be induced at room temperature. By heating over 70 °C, the polymers became more fluid and the samples remained highly birefringent until 150 °C. At higher temperatures, the polymers started to decompose. The textures observed in the liquid crystalline phase were not the classical and characteristic textures of smectic or nematic mesophases.

The DSC studies of both the pPYCOOC12 and pPYOC12 showed no melting and no crystallization down to −120 °C, but did show a reversible weak enthalpy transition at about 70 °C. Those results were corroborated by the observation that showed some more fluid states for temperatures higher than 70 °C but still birefringence.

Figure 7 shows the X-ray scattering patterns obtained for pPYCOOC12 at room temperature (top) and 80 °C (bottom). A diffuse Bragg reflection at large angles and a sharp band at small angles are clearly observed, whose corresponding periodicities are about 4.5 Å for the diffuse reflection and 26 Å for the sharp band. A sharp diffraction ring of low intensity could be also observed at wide angle, corresponding to a periodicity of 3.59 Å. The diffraction diagrams of Figure 7, obtained successively at room temperature and in the fluid birefringent phase at 80 °C, show clearly at small angles a sharper diffraction ring at 80 °C than at room temperature, which indicates an increase of the order in the fluid phase. The sharpness of the diffraction rings in the liquid crystalline phase of Figure 7b suggests also that the mesophase of pPYCOOC12 has a lamellar order, similar to the molecular organization of a smectic mesophase. Unfortunately, no specific texture can be clearly identified from optical microscopy to confirm this mesophase. For pPYOC12 the diffraction patterns are similar to the previous one. A sharp diffraction ring is observed at low angle and only a diffuse halo at wide angle. These results suggest the same lamellar order.

2.2.4. Orientation. The liquid crystal properties enabled the orientation of the polymers by shearing or methods such as thermal gradient. Through thermal scanning by a laser beam at the absorption band wavelength of the polymer (488 nm), a rather good orientation

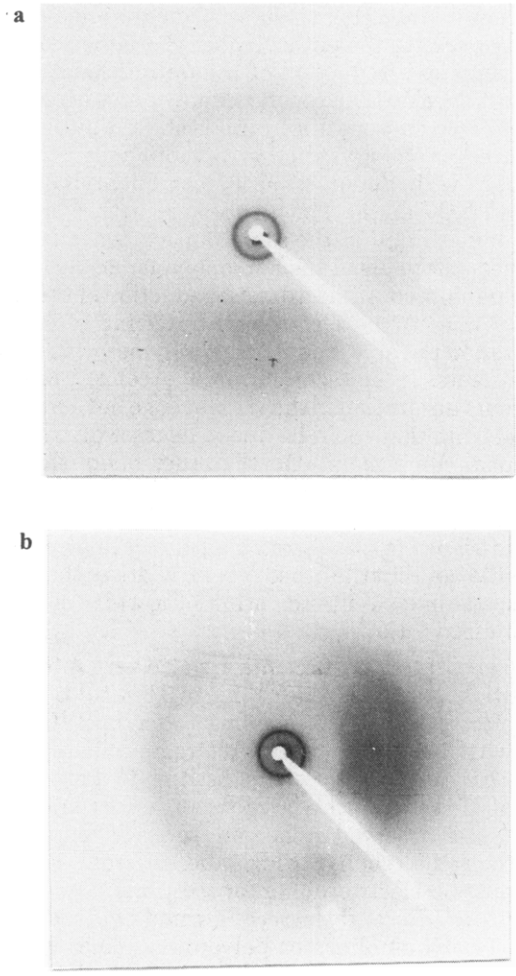

Figure 7. X-ray scattering patterns of pPYCOOC12 (top) at room temperature and (bottom) at 80 °C.

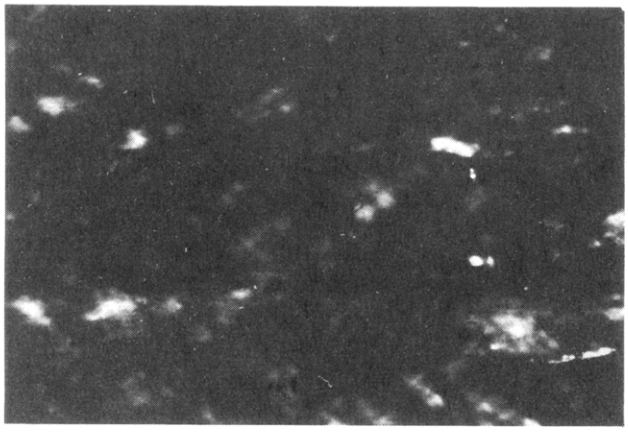

Figure 8. Optical micrograph between crossed polarizers of partially oriented film by shearing at 90 °C between fused quartz plates.

of the heating zone was shown.[14] Figure 8 shows the birefringence of the highly red colored pPYOC12 film observed by optical microscopy and partially oriented under shear at 70 °C. The observation between crossed polarizers revealed in red the oriented microdomains in the direction of shear. Figure 9 shows the optical dichroism of a thin oriented film in the UV–vis range for different angles of the polarized incident light. The two extreme curves are obtained for the polarizations parallel and perpendicular to the shear axis. A broad absorption peak is centered on 485 nm with a shoulder at 450 nm as observed in unpolarized light. The other extreme curve, corresponding to the perpendicular direction of observation, shows a much lower absorption band with a large attenuation and a poor resolution of the peak at 485 nm.

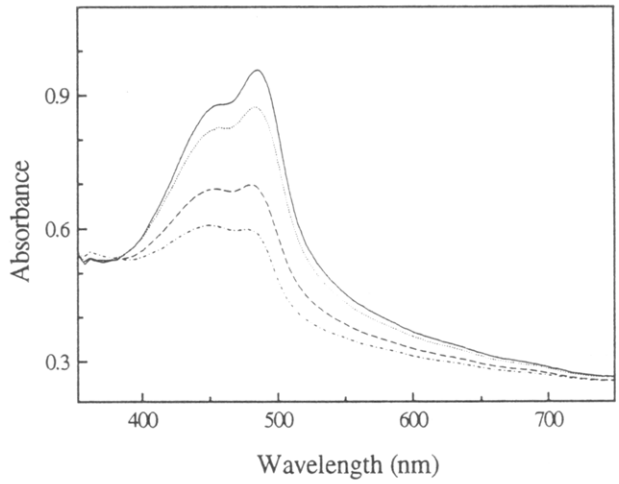

Figure 9. UV–vis dichroism spectra on pPYOC12 thin films for some different orientation angles of the polarizer. The polarizer angles correspond to 0 (—), 30 (···), 60 (— –), and 90° (– –) with respect to the shear axis of the polymer.

3. Discussion

3.1. Polymer Chain Characterization. The polycondensation of substituted diethynyl aryl derivatives by a Pd-coupling method affords a class of soluble rigid and conjugated polymers of high molecular weight. The average molecular weight of a phenylene disubstituted by a long aliphatic side chain reaches a value of 10^5, i.e., 10^2 times more than synthesized oligomers of ref 7, in which the aryl group of the backbone was unsubstituted. More recently, the coupling reaction was applied to the phenyl rings carrying long side chains in order to increase the solubility of these conjugated polymers. Long flexible chains increase the solubility and the molecular weights up to 10^4. Our experimental conditions, slightly different, are milder and afford some difference in the solvent or in the catalysts. The polycondensation method was carried out in a mixture of triethylamine and tetrahydrofuran at 85 °C, with $PdCl_2$, PPh_3, $CuAc_2$ acting as catalysts. The reaction was done in THF as cosolvent which is well known for its solvatation properties of metal complexes and the good solubilization of more or less polarizable chains.

The solubility of the polymers depends on the number and length of the side chain on aryl groups. All samples are found to be of high molecular weight. By GPC long polymer chains are detected with M_w of the longest chains up to 5×10^5. The solubility of substituted aryl polymers depends on the number and the length of the side chain (ether or esters) > unsubstituted oligomers.[6,7] Copolymers such as anthryl–phenyl diethers, which carry unsubstituted aryl groups as alternating units, are less soluble in solvents such as THF or CH_2Cl_2 than substituted homopolymers with the same flexible chain.

The light-scattering measurements on-line method, already described in previous papers,[11] demonstrates its utility in this work. The light-scattering detection method of molecular weight (hereafter LS M_w) gives the weight average molecular weight of these very rigid chains, which cannot be obviously deduced from PS calibration method. As compared with the molecular weight determinations of Giesa and Schultz,[15] our measurements (LS M_w) show M_w values 1 order higher than in the previous work. We found one distribution peak centered on 10^5 for the diether

derivative, while the cited authors found, by extrapolating the correlated elution volume and calculated masses of the shortest oligomers from the TB method with PS calibration, two main oligomer peaks at 5×10^3 and 1×10^4 (method A). As we found that even for very low molecular weights, the PS calibration method cannot be applied to these polymers, the calculated masses of their oligomers are probably inaccurate. For the B method, the distribution is shifted to higher M_w's and the polymers become insoluble after drying, indicating a cross-linking of polymer samples. From GPC measurements on crude polymers a large molecular weight distribution occurs ($M_w/M_n = 1.89$). The samples include in low content the monomer residue and the shortest oligomers (dimers or trimers), which could be considered as impurities related to the average molecular weight of 10^5 and to the longest characterized chains (5×10^5). Moreover, for the optical applications it is well known that the third-order susceptibility of the tolan and their derivatives is essentially low.[16] Thus, by use of a GPC preparative column, the oligomeric fraction could be easily removed from crude preparation. With the increase of their weight average molecular weight the polymers of this work become less soluble and their solubilization takes a long time at room temperature after drying.

The stiffness of the chain in solution in THF using the principle of universal calibration shows an unusual coefficient of the slope in the Mark–Houwink representation ($\alpha = 1.92$). The exponent α, larger than those of usual semirigid chains (i.e., $\alpha = 0.90$–1.00 for substituted PA in THF), proves that the polymers in solution are in a fully rigid conformation. Such values of the exponent have been found already in one of the most rigid poly(benzothiazole) homopolymers (PBT) with catenation angles of nearly 180°.[12b]

The value of the average root mean square radius of gyration of the chain in the THF solvent was 630 Å. This value, calculated from the Zimm plot, was consistent with a perfectly extended rod chain. From the weight average molecular weight $\langle \bar{M}_w \rangle = 10^5$, we calculate a $\langle \mathrm{DPn} \rangle = 213$ and a mean length of an extended rigid chain equal to 1530 Å (with a monomer length of 7.2 Å). From this length the calculated value of the gyration radius of a rigid rod chain $\langle R^2_g \rangle^{1/2} = (L^2/12)^{1/2}$ is equal to 440 Å, slightly lower than the former value, calculated from the Zimm plot, and which does not take into account in the same manner the molecular distribution.

3.2. Optical Properties. The absorption spectra of the polymer solutions show a typical absorption band, in the visible range 400–510 nm, very different from the large and structured polydiacetylene absorption band. In the near-UV a slightly low absorption band or a shoulder is shown at 300–320 nm. These absorption bands are different from these of the aryl–diethynyl monomers (Figure 3a). A noticeable difference in the absorption spectra of polymer solutions or of thin solid films is also shown in the series of homo- or copolymers, according to the electron-withdrawing or -donating character of the aryl substituent. The induced perturbations, depending on the electronegativity of the group, are largely observable on the spectroscopic data in Table 1. For the homopolymer based on aryl diether, where the ether is a moderated electron-donor group, the absorption peak is centered on 455 nm (2.72 eV). With an acceptor group such as the monoester, the homopolymer shows a blue shift by 50 nm of the absorption peak. For alternated copolymers with an electron-rich unit a red shift is observed. A significant red shift by 68 nm of the main peak centered at 521 nm is shown from the phenyl–diether homopolymer to the anthryl–phenyl–diether copolymer, which implies a reduction of the optical band gap from 2.72 to 2.38 eV. The second copolymer with a stilbene unit as electron-donating group is shifted by only 16 nm compared to the aryl–diether homopolymer. Other copolymers with donor or acceptors on aryl-alternating groups. NO_2–diether, or monoester–diether are successively blue shifted in the same range of wavelength (412 nm), near the value of the homopolymer aryl–monoester. The blue shift confirms a drastic reduction of the electron density due to the electron-withdrawing effect of the acceptor on the aryl groups. The polymer with thioether substituents, in spite of its orange color, presents no maximum absorption in the visible range but a broad band until 450 nm that could be due to a larger distribution of rotational conformers. On the other hand, the Raman spectra of this polymer and an aryl diether polymer (Figure 5b) show very close maxima (2199 and 2196 cm^{-1}) for the bands assigned to C≡C stretching, indicating a quite good delocalization, but the broader band width of the thioether polymer is indeed an indication of a wider conjugation length distribution.

The absorption coefficients are also very interesting, ϵ in solution increases from 7×10^3 to 3.6×10^4 L mol^{-1}, i.e., log ϵ from 3.8 to 4.5, passing from cpPYOC12A to pPYCOOC12, which suggests a larger oscillator strength for the pPY chain with ester substituents than with other groups. However, such a large dispersion of the absorption coefficients, observed in the same series of homopolymers with the same ethynyl bridge and different substituted aryl groups as electron donors or acceptors, *is not perfectly understood*. Recently, new conjugated rigid rod polymers such as polyquinolines or polyanthrazolines containing an ethynyl bond were investigated.[17] The band gaps of these films are found to be between 2.5 and 2.0 eV, while the absorption coefficients or the log ϵ values were in the range of 4.6–4.9. We expect that the high values of ϵ, in pPy, induced by the large oscillator strength of the triple bond and more or less the π electron delocalization, will be related to the high values of the nonlinear susceptibility, through the transition dipole moment and the inverse of the sixth power of the band gap energy.[18] The authors of ref 17 found in the series of polyquinolines or polyanthrazolines that the magnitude of the resonant or nonresonant $\chi^{(3)}$ could not be correlated with the optical band gap of π-electron delocalization.[19] They used a three-level model based on essential states, which fits well with the $\chi^{(3)}$ dispersion to suggest that more than one excited state is responsible for the third-order nonlinearity of the polymers. We expect also, in the polymer series of this work, to find larger values of resonant or nonresonant $\chi^{(3)}$ than for the first ether derivative[14] for the highest oscillator strength and the smallest band gap of this class of polymers. The third-order optical measurements of this series of polymers are in progress.

3.3. Thermal Properties and Orientation. The thermal stability observed by thermal analysis under air or nitrogen of the substituted series of pPY is obviously not as large as that of the unsubstituted product given in the literature[7] but also was not as stable as the other substituted alkyl–ether homopolymers.[15] In this work the disubstituted phenyl chain already shows a small weight loss at 220 °C in N_2, while in the referenced paper[7] the decomposition does not begin before 300 °C. pPY with ester substituents shows weaker thermal stability. As shown in Figure 6 a two-step weight loss is also detected; the first step was attributed to the split off of the side

chain and a second step attributed to the total oxidation of the chain. In this work we find a greater thermal sensitivity at milder temperature than previous polymers, and at higher temperature, in the range of 350–800 °C, the second decomposition step is in good agreement with the literature data.

X-ray Discussion. The low-angle X-ray diffractograms of the pPYCOOC12 and pPYOC12 show a characteristic pattern of a lamellar structure often observed for rigid-rod polymer with flexible side chain.[20] The interplanar spacing calculated from small-angle diffraction of 26 Å for pPYCOOC12 and 27 Å for pPYOC12 is not in agreement with the calculated length of the lateral groups in an extended conformation. These results imply for the lateral substituents a lamellar organization of the paraffinic chains with a partial interdigitation of the ends.

Orientation from Isotropic Film to Oriented Film. As seen by optical microscopy, the fresh films prepared by casting are perfectly isotropic, while the film becomes highly oriented by shearing or stretching. Although applied to the melt phase (80–90 °C) the shear method induces numerous small domains, characterized by a high birefringence and random orientation. This poor organization of the films could be due to the very high viscosity of the polymer in the LC phase and/or relaxations during the freezing.

Other attempts in the orientation methods have been attempted, such as orientation in the thermal gradient induced by absorption of a laser beam.[14] The exploration of all experimental conditions of laser-induced orientation are in progress.

4. Conclusions

In this work we have been able to prepare a series of rigid rod conjugated polymers starting from arylethynylene basic units with various side chains in order to increase the polymer solubilities. We presented for the first time a complete characterization of poly(phenylethynylene) derivatives bearing alkoxy groups and long hydrocarbons tails of 10 and 12 carbon atoms. The characterization by GPC of the polymer substituted with two dodecyl ether chains on the phenyl group shows the highest average molecular weight ever synthesized on this type of homopolymer, finding a value as high as 10^5 g/mol. We compare this model polymer with other new polymers, a homopolymer based on the phenyl unit bearing an electron-acceptor group such as an alkyl ester, or copolymers based on the phenyl alcoxy unit and other electron-donor groups, such as anthryl, thienyl, or stilbene units. The spectroscopic linear properties in solution and in solid thin films confirm a large shift of the main absorption peak of the π–π^* transition in the visible range according to the donor or acceptor character of the substituent or comonomer group. Studies by Raman spectroscopy of the alkoxy derivative homopolymer and the corresponding trimer show a shift of the triple bond's stretching band, and so a greater delocalization for the polymer. Highly birefringent liquid crystalline phases are induced by rubbing or shearing, which are confirmed by an observation of the optical dichroism along the shearing direction.

5. Experimental Section

5.1. Materials. We have synthesized a series of diethynylaryl monomers, which were then polymerized with dibromoaryl units using the organic Pd-coupling reaction. The dibromomethoxyanisole (1), iodine, bromoalkanes, dicyclohexylcarbodiimide (DCCI), (trimethylsilyl)acetylene (TMSA), palladium(II) chloride ($PdCl_2$), triphenylphosphine (PPh_3), potassium carbonate (K_2CO_3), and sodium iodide (NaI) were obtained from Lancaster. The 2,5-dibromobenzoic acid 3, (dimethylamino)pyridine (DMAP), chlorosulfonic acid ($ClSO_3H$), 4-hydroxypiperidine, zinc, copper(II) acetate ($CuAc_2$), methylene chloride (CH_2Cl_2) HPLC grade, tetrabutylammonium fluoride (TBAF) 1.1 M in THF, and aluminum powder were obtained from Aldrich and used without further purification. Triethylamine (Aldrich) was distilled from KOH before use. Toluene and THF were distilled from Na and kept under N_2.

5.2. Synthesis Methods. Synthesis of 1,4-Dibromo-2,5-dialkoxybenzene. The dibromodialkoxybenzene was prepared by cleaving the methoxy substituents of a dibromomethoxyanisole using aluminum iodide as reagent[21] and then alkylation of the phenol functions. The synthesis is described for the dibromodidodecanoxybenzene, following the reaction

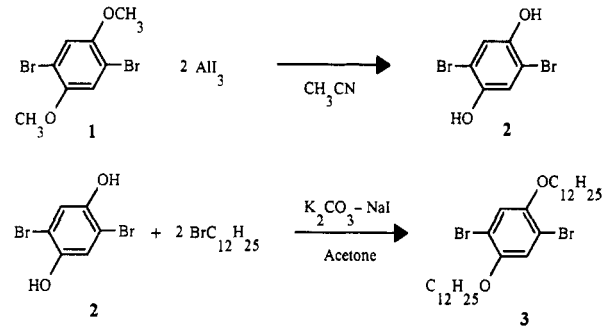

2,5-Dibromohydroquinone (2).[21] In a cooled vessel at 10 °C were mixed 40 mL of dry acetonitrile, aluminum powder (1.349 g, 50 mmol), and iodide (9.518 g, 75 mmol). The mixture was then slowly warmed to reflux with stirring, and the reaction was pursued until the violet color of the iodide disappeared after 30 mn.

To the freshly prepared mixture of AlI_3 (1.25 M, 40 mL, 50 mmol) was added the dibromomethoxyanisole (5.919 g, 20 mmol), with 20 mL of acetonitrile, and the resulting mixture was then refluxed and stirred for 24 h. The suspension was cooled and poured in aqueous HCl solution (0.5 M, 100 mL). The mixture was extracted first with ether, and then the etherate phase was extracted with a 5% solution of sodium hydroxide. The aqueous solution was acidified with HCl and then extracted with ether. The solution was dried over Na_2SO_4 and the solvent was removed. After chromatography (silica gel, heptane/CH_2Cl_2 (1/1)) 4.311 g of pure dibromohydroquinone was obtained (yield 80%): ^{1}H NMR ($CDCl_3$) δ 8.65 (s, 2H, OH), 7.15 (s, 2H, arom). Anal. Calcd: C, 26.86; H, 1.49; O, 11.94. Found: C, 26.93; H, 1.43; O, 12.03.

Dibromobis(dodecyloxy)benzene (3).[22a] To the dibromohydroquinone (2.679 g, 10 mmol) in 100 mL of acetone was added potassium carbonate (2.764 g, 20 mmol), 1-bromododecane (4.985 g, 20 mmol), and sodium iodide (15 mg, 0.1 mmol), and the resulting mixture was then refluxed until no more starting material could be detected by TLC. After filtration, the solvent was removed and the residue was dissolved in ether and washed with a KOH aqueous solution (0.1 M). After drying, the solvent was evaporated. The crude product was purified by chromatography (SiO_2, CH_2Cl_2/heptane (1/2)): yield 60%; ^{1}H NMR ($CDCl_3$) δ 7.25 (s, 2H, arom), 4.05 (t, 4H, OCH_2), 1.8 (q, 4H, CH_2 β ether), 1.3 (36 H, CH_2), 0.9 (t, 6H, CH_3). Anal. Calcd: C, 59.60; H, 8.60; O, 5.29. Found: C, 59.70, H, 8.33, O, 5.57.

The same method was used to synthesize dibromobis(decyloxy)benzene (4): yield 82%; ^{1}H NMR ($CDCl_3$) δ 7.26 (s, 2H, arom), 4.06 (t, 4H, OCH_2), 1.8 (q, 4H, CH_2 β ether), 1.3 (28 H, CH_2), 0.9 (t, 6H, CH_3).

Synthesis of 2,5-Dibromododecylbenzoate (6). The 2,5-dibromobenzoic acid (5) was esterified with dicyclocarbodiimide (DCC) and 4-(dimethylamino)pyridine (DMAP) in methylene chloride alcohol free as described:[23]

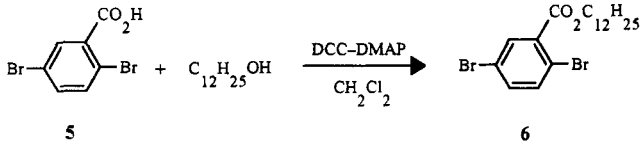

Dibromobenzoic acid (5) (2.799 g, 10 mmol), dodecanol (1.863 g, 10 mmol), DCCI (3.0945g, 15 mmol), and DMAP (100 mg, 0.82 mmol) were charged in a single-necked flask topped with a calcium chloride guard tube and stirred for 15 h. Urea was filtered off and the filtrate washed with a 0.5 M HCl solution and then with a saturated $NaHCO_3$ solution. The solution was dried on Na_2SO_4, the solvent was removed, and the crude product was chromatographed (SiO_2, CH_2Cl_2/heptane (1/1)): yield 85%; ^1H NMR ($CDCl_3$), δ 7.9 (d, 1H, arom), 7.5 (d, 1H, arom), 7.43 (dd, 1H, arom), 4.35 (t, 2H, $COOCH_2$), 1.8 (q, 2H, CH_2 β ester), 1.3 (18H, CH_2), 0.9 (t, 3H, CH_3). Anal. Calcd: C, 50.89, H, 6.25, O, 7.14. Found: C, 51.42; H, 6.18; O, 6.78.

2,5-Dibromobenzenesulfonyl Chloride (8).[22b] In a cooled vessel were charged the *p*-dibromobenzene (7) (9.437 g, 40 mmol) and the chlorosulfonic acid (8 mL, 120 mmol). The mixture was stirred for 3 h and then poured onto 50 mg of ice and rapidly extracted with methylene chloride. The solvent was removed to obtain 10.7 g of 2,5-dibromobenzenesulfonyl chloride, yield 80%.

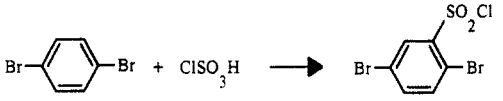

7 8

2,5-Dibromothiophenol (9).[22c] The 2,5-dibromobenzenesulfonyl chloride (8) (10.031 g, 30 mmol) was placed in a two-necked flask equipped with a condenser and a separatory funnel and immersed in a freezing mixture of ice and salt to maintain the temperature under 0 °C. One hundred mL of sulfuric acid was slowly poured, zinc powder (12 g, 184 mmol) was added, and the cooled mixture was stirred for 1 h and then warmed to reflux until the solution became clear. The mixture was cooled, and thiophenol was filtered and purified by chromatography (SiO_2, CH_2Cl_2/heptane (2/1)). A total of 6.673 g of pure thiophenol was obtained: yield 83%; ^1H NMR (acetone-d_6), δ 7.74 (d, 1H, arom), 7.48 (d, 1H, arom), 7.23 (dd, 1H, arom), 4.93 (s, 1H, SH).

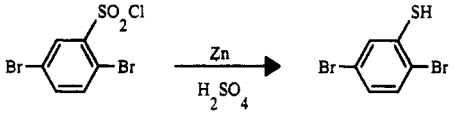

8 9

2,5-Dibromo(dodecylthio)benzene (10): The dibromothiophenol (9) (2.679 g, 10 mmol), K_2CO_3 (1.382 g, 10 mmol), and the 1-bromododecane (2.492 g, 10 mmol) were placed in a vessel with 100 mL of acetone and warmed to reflux, following the synthesis described for dibromodialkoxybenzene.[22a] yield 90%; ^1H NMR ($CDCl_3$) δ 7.38 (d, 1H, arom), 7.30 (d, 1H, arom), 7.13 (dd, 1H, arom), 2.93 (t, 2H, SCH_2), 1.71 (q, 2H, CH_2 β ether), 1.29 (18 H, CH_2), 0.89 (t, 3H, CH_3). Anal. Calcd: C, 49.55; H, 6.47. Found: C, 49.83; H, 6.33.

2,5-Dibromo-4-(4-hydroxypiperidinyl)toluene (11). The 2,5-dibromo-4-fluorotoluene (10) (5.359 g, 20 mmol), 4-hydroxypiperidine (5.058 g, 50 mmol) and potassium carbonate (1.382 g, 10 mmol) were charged with 8 mL of dimethyl sulfoxide in a vessel equipped with a reflux condenser and a magnetic stirrer. The mixture was heated to 110 °C for 72 h. The cooled mixture was then poured into cold water and stirred for 1 h. The precipitate was collected by filtration, and the derivative was purified by chromatography (SiO_2, CH_2Cl_2) to obtain 3.304 g of pure product: yield 45%; ^1H NMR ($CDCl_3$), δ 7.43 (s, 1H, arom), 7.20 (s, 1H, arom), 3.85 (m, 1H, CHOH), 3.24 (m, 2H), 2.77 (m, 2H), 2.31 (s, 3H, CH_3), 2.01 (m, 2H), 1.80 (m, 2H), 1.59 (m, 1H, OH). Anal. Calcd: C, 49.55; H, 6.47. Found: C, 49.83; H, 6.33.

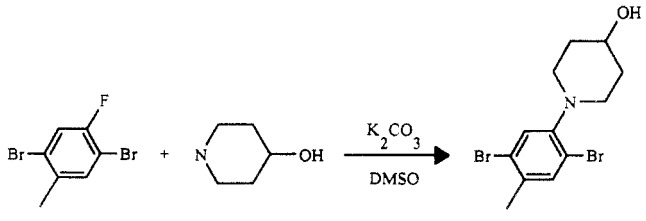

11

Synthesis of the 1,4-Diethynylaryls 16. The synthesis is described for one diethynyl monomer. The same procedure is used for all the diethynyl compounds.[9,10]

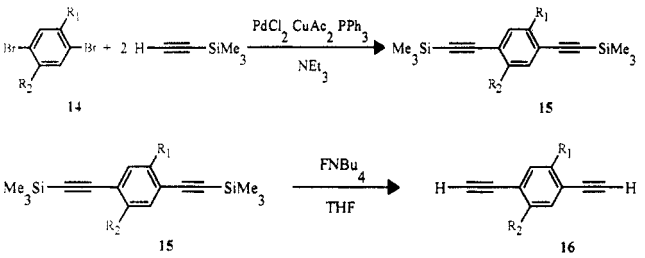

1,4-Bis[(trimethylsilyl)ethynyl]-2,5-bis(dodecyloxy)benzene (15). Palladium chloride (53 mg, 0.30 mmol), copper acetate (60 mg, 0.3 mmol), triphenylphosphine (262 mg, 1.0 mmol), and the dibromobis(dodecyloxy)benzene (14) (1814 mg, 3.2 mmol) were charged under nitrogen in a two-necked flask with dry and degassed triethylamine (100 mL). (Trimethylsilyl)acetylene (1.5 mL, 10.6 mmol) was added and the reaction mixture was stirred and heated at 85 °C under nitrogen for 8 h. After being cooled at room temperature, the mixture was filtered to eliminate the ammonium salt and the triethylamine was removed. The soiled residue was dissolved in dichloromethane, recrystallized in methanol, and then purified by chromatography (SiO_2, CH_2Cl_2/heptane (1/2)), 1.630 g; yield 85%.

1,4-Diethynyl-2,5-bis(dodecyloxy)benzene (16).[24] The bis[(trimethylsilyl)ethynyl]bis(dodecyloxy)benzene 15 (1.278 g, 2 mmol) was dissolved in 50 mL of tetrahydrofuran, and a solution of tetrabutylammonium fluoride (1.1 M, 1 mL, 1.1 mmol) was added. After stirring for 5 min at ambient temperature, the mixture was chromatographed on a small silica gel column using tetrahydrofuran as eluent. The solvent was removed, and the crude product was recrystallized in methanol and dried in vacuo.

Diethynylbis(decyloxy)benzene: yield 95%; ^1H NMR ($CDCl_3$) δ 6.95 (s, 2H, arom), 3.95 (t, 4H, OCH_2), 3.34 (s, 2H, CCH), 1.8 (q, 4H, CH_2 β ether), 1.3 (28 H, CH_2), 0.9 (t, 6H, CH_3). Anal. Calcd: C, 82.14; H, 10.57; O, 7.29. Found: C, 82.07; H, 10.61; O, 7.33.

Diethynyldodecylbenzoate: yield 65%; ^1H NMR ($CDCl_3$) δ 8 (s, 1H, arom), 7.56 (d, 2H, arom), 4.35 (t, 2H, OCH_2), 3.5 (s, 1H, CCH), 3.2 (s, 1H, CCH), 1.75 (q, 2H, CH_2 β ester), 1.3 (18 H, CH_2), 0.9 (t, 3H, CH_3). Anal. Calcd: C, 81.61; H, 8.93; O, 9.45. Found: C, 81.18; H, 9.08; O, 9.23.

Polymerization was performed by Heck coupling, using a palladium complex as catalyst.[9,10]

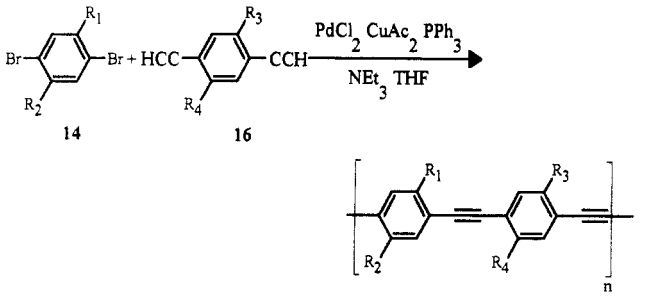

The monomers (1.8 mmol of each), palladium chloride (35 mg, 0.2 mmol), copper acetate (6 mg, 0.03 mmol), triphenylphosphine (210 mg, 0.8 mmol), triethylamine (100 mL), and tetrahydrofuran (30 mL), all dry and degassed, were put under nitrogen in a two-necked 250-mL flask equipped with a magnetic stirrer and a reflux condenser. For the copolymer pPYOC12A was charged with 30 mL of toluene instead of THF. The degassed reaction mixture was heated at 85 °C and stirred under nitrogen for 3 days. The precipitated ammonium salt was filtered off and washed with THF, keeping the organic phases together. The solvents were removed, and the residue was dissolved in 5 mL of hot THF, poured in to 200 mL of cold methanol to precipitate, centrifuged, and then dried in vacuo. The remaining monomers and smallest oligomers were removed by preparative GPC to obtain a red-orange fluorescent polymer. The yields varied

between 35 and 80%. The polymers were characterized by ^{1}H and ^{13}C NMR.

5.3. Instruments and Characterization Methods. The polymer molecular weights were obtained by gel permeation chromatography (GPC) in eluent THF with the coupled detection of refractive index and light scattering on a previously described apparatus.[11] The infrared spectra of thin solid films deposited on KBr plates were recorded on a Perkin-Elmer 983 infrared spectrophotometer, and the ultraviolet absorption spectra were measured in THF solution or in cast solid films on quartz substrates with a Shimadzu UV-2101PC UV–vis scanning spectrophotometer. Fluorescent measurements were performed on a Hitachi F4010 apparatus. Raman scattering measurements were performed with a 1061-nm Nd–Yag laser line and a Brüker FTIR spectrometer (IFS 66 and FRA 106), which were described elsewhere.[25]

Differential scanning calorimetry (DSC) was performed on a Perkin-Elmer DSC7. The melting points were determined on an electrothermal digital melting point apparatus or by DSC. Thermogravimetric analyses were realized with a Mettler TA3000 system.

^{1}H and ^{13}C NMR spectra were obtained in $CDCl_3$ with a Brüker AC-200F spectrometer at rt or with a variable-temperature probe.

The molecular modeling was performed with Sybyl software from Tripos, running on a DEC Vax unit linked with a graphic unit from Evans and Sutherland.

Acknowledgment. The authors are grateful to Dr. C. Strazielle for the GPC measurements and for the helpful discussions on polymers in solution, to B. Heinrich for X-ray diffraction measurements, and L. Oswald for the chemistry assistance. We thank also M. Taylor and P. McNeillis for the English corrections.

References and Notes

(1) Yu, L.; Dalton, L. R. *Macromolecules* **1990**, *23*, 3439.
(2) Rehahn, M.; Schlüter, A. D.; Wegner, G. *Makromol. Chem.* **1990**, *191*, 1991.
(3) Rutherford, D.; Stille, J. K.; Elliott, C. K.; Reichert, V. R. *Macromolecules* **1992**, *25*, 2294.
(4) Sasabe, H.; Wada, T.; Hosoda, H.; Ohkawa, H.; Yamada, A.; Garito, A. F. *Mol. Cryst. Liq. Cryst.* **1990**, *189*, 155.
(5) Lakmikantham, M. V.; Vartikar, J.; Kwan, Y. J.; Cava, M. P.; Huang, W. S.; MacDiarmid, A. *Polym. Prep.* **1983**, *24*, 75.
(6) Sanechika, K.; Yamamoto, T.; Yamamoto, A. *Bull. Chem. Soc. Jpn.* **1984**, *57*, 752.
(7) Trumbo, C.; Marvel, S. *J. Polym. Sci., Polym. Chem.* **1986**, *24*, 2231.
(8) Heck, R. F. *Palladium Reagents in Organic Syntheses*; Academic Press: New York, 1990; p 299.
(9) Dieck, H. A.; Heck, R. F. *J. Organomet. Chem.* **1975**, *93*, 259.
(10) Austin, W. B.; Bilow, N.; Kelleghan, W. J.; Lau, K. S. Y. *J. Org. Chem.* **1981**, *46*, 2280.
(11) Beltzung, L.; Strazielle, C. *Makromol. Chem.* **1984**, *185*, 1155.
(12) (a) Lowell, P. A. In *Comprehensive Polymer Science: Dilute solution viscometry*; Allen, G., Bevington, J. C., Eds.; Pergamon Press: New York, 1989; Vol. 1, p 190. (b) Wolfe, J. F. *Encyclopedia of Polymer Science & Eng.*, 2nd ed.; John Wiley & Sons: New York, 1988; Vol. 11, p 622.
(13) (a) Zheng, R. X.; Benner, R. E.; Vardeny, Z. E.; Baker, G. I. *Phys. Rev. B, Rapid Commun.* **1990**, *42*, 3235. (b) Tian, B.; Zerbi, G.; Schenk, R.; Mullen, K. *J. Chem. Phys.* **1991**, *95*, 3191.
(14) Le Moigne, J.; Moroni, M.; Coles, H.; Thierry, A.; Kajzar, F. *Mat. Res. Soc. Symp. Proc.* **1992**, *247*, 65.
(15) Giesa, R.; Schultz, R. *Makromol. Chem.* **1990**, *191*, 857.
(16) Perry, J. W.; Stiegman, A. E.; Marder, S. R.; Coulter, D. R.; Beratan, D. N.; Brinza, D. E.; Klavetter, F. L.; Grubbs, R. H. *Nonlinear Optical Properties of Organic Materials, SPIE Proc.* **1988**, *971*, 17.
(17) Agrawal, A. K.; Jenekhe, S. A.; Vanherzeele, H.; Meth, J. S. *Polym. Prep.* **1991**, *32*, 124. Agrawal, A. K.; Jenekhe, S. A. *Macromolecules* **1991**, *24*, 6806.
(18) (a) Agrawal, G. P.; Cojan, C.; Flitzanis, C. *Phys. Rev. B.* **1978**, *17*, 776. (b) Rustagi, K. C.; Ducuing, J. *Optics Commun.* **1974**, *10*, 258.
(19) Agrawal, A. K.; Jenekhe; Vanherzeele, H.; Meth, J. S. *J. Phys. Chem.* **1992**, *96*, 2837.
(20) Ballauf, M.; Schmidt, G. F. *Mol. Cryst. Liq. Cryst.* **1987**, *147*, 163.
(21) Vivekananda Bhatt, M.; Ramesh Babu, J. *Tetrahedron Lett.* **1984**, *25*, 3497.
(22) Vogel, A. I. *Textbook of Practical Organic Chemistry*, 4th ed.; Logman: Birmingham, (a) p 754; (b) p 647; (c) p 656.
(23) Neises, B.; Steglich, W. *Angew. Chem., Int. Ed. Engl.* **1978**, *7*, 52.
(24) Nakamaru, E.; Kuwajima, I. *Angew. Chem., Int. Ed. Engl.*, **1976**, *15*, 498.
(25) Botta, C.; Luzzati, S.; Tubino, R.; Borghesi, A. *Phys. Rev. B* **1992**, *46*, 13008.